

# A Turbulent Heating Model Combining Diffusion and Advection Effects for Giant Planet Magnetospheres

C. S. Ng<sup>1</sup>, B. R. Neupane<sup>1</sup>, P. A. Delamere<sup>1</sup>, P. A. Damiano<sup>1</sup>

<sup>1</sup>Geophysical Institute, University of Alaska Fairbanks, Fairbanks, AK, USA

## Key Points:

- A new and improved model for the heating of the magnetospheres of Jupiter and Saturn by magnetohydrodynamic turbulence is developed
- The model combines effects from diffusion and advection such that each is dominant when the radial flow velocity is small or large
- Predictions of the temperature and radial flow velocity profiles agree better with Jupiter and Saturn observations than previous models

arXiv:2110.08767v1 [physics.space-ph] 17 Oct 2021

---

Corresponding author: C. S. Ng, [cng2@alaska.edu](mailto:cng2@alaska.edu)

**Abstract**

The ion temperature of the magnetospheres of Jupiter and Saturn was observed to increase substantially from about 10 to 30 planet radii. Different heating mechanisms have been proposed to explain such observations, including a heating model for Jupiter based on MHD turbulence with flux-tube diffusion. More recently, an MHD turbulent heating model based on advection was shown to also explain the temperature increase at Jupiter and Saturn. We further develop this turbulent heating model by combining effects from both diffusion and advection. The combined model resolves the physical consistency requirement that diffusion should dominate over advection when the radial flow velocity is small and vice versa when it is large. Comparisons with observations show that previous agreements, using the advection only model, are still valid for larger radial distance. Moreover, the additional heating by diffusion results in a better agreement with the temperature observations for smaller radial distance.

**Plain Language Summary**

The ion temperature of the magnetospheres of Jupiter and Saturn was observed to increase substantially near the planet. This suggests that there should be some heating sources to counter the cooling effect due to expansion. There have been several models trying to explain such observation using different heating mechanisms, including a heating model for Jupiter based on turbulence and diffusion effects, as well as a model based on advection effects for Jupiter and Saturn. We further develop a heating model by combining effects from both diffusion and advection. The combined model resolves the physical consistency requirement that diffusion should be stronger than advection nearer to the planet, but shifting to the opposite farther away. Comparisons with observations show that previous agreements using the advection only model are still valid, and are improved by including diffusion nearer to the planet.

**1 Introduction**

One major unresolved problem in the physics of giant magnetospheres is to find the mechanism responsible for the observed increase of ion temperature with radial distance (e.g., Bagenal & Delamere, 2011). Such observations show that the ion temperature of the magnetospheres of Jupiter and Saturn increase substantially, about a factor of 3, from about 10 to 30 planet radii. This suggests that there should be some heating sources to counter the cooling effect due to adiabatic expansion. There have been several models proposed to explain such observations using different heating mechanisms (e.g., Hill et al., 1983). Saur (2004) considered the possibility of turbulent heating of Jupiter’s magnetodisc (10 to 40  $R_J$ ) based on magnetohydrodynamic (MHD) turbulence, and flux tube diffusion. Another turbulent heating model for Jupiter was developed by Ng et al. (2018), in which the outward plasma transport is dominated by advection rather than diffusion, as inspired by turbulent heating models of the solar wind (e.g., Ng et al., 2010). They found that the observed heating rate density due to MHD turbulence can provide enough heating to explain the observed increase of ion temperature to about 30  $R_J$ . More recently the same turbulence heating model was also applied to Saturn’s magnetosphere by Neupane et al. (2021), who also found a consistent relationship between the heating rate density and the temperature increase.

The justification for the advection dominated turbulent heating model was argued in details by Ng et al. (2018), based on the observed fact that beyond about 10  $R_J$  the radial transport time becomes much shorter, or the radial outflow speed becomes much larger (Delamere & Bagenal, 2010; Bagenal & Delamere, 2011; Bagenal et al., 2016). While this model does give the required heating rate at the radial positions up to about 30 planet radii for both Jupiter and Saturn, strictly speaking it cannot be applied to positions near and inward of 10 planet radii due to the fact the the radial outflow speed is still small

there. Moreover, the temperature increases predicted by this model do seem to be significantly smaller than the observed data for both Jupiter and Saturn in the near planet positions (Ng et al., 2018; Neupane et al., 2021).

In this paper, we develop a new turbulent heating model by combining the diffusion model of Saur (2004), and the advection model of Ng et al. (2018). The formulation for this model will be given in the next Section. In Section 3 we will apply this new model to both Jupiter and Saturn cases to compare the predicted temperature, as well as radial outflow speed, with observations. Discussion and conclusion will be given in Section 4.

## 2 A Combined Turbulent Heating Model

We start the derivation of the one-dimensional steady-state turbulent heating model by writing down the transport equations for mass,

$$\dot{M} = 2\pi LRHm_inV_r - 2\pi m_i \frac{D_{LL}}{L^2} \frac{d}{dL} (nHL^3). \quad (1)$$

In this equation,  $\dot{M}$  is the mass rate to be transported out of the inner magnetosphere injected by Io of Jupiter or Enceladus of Saturn.  $R$  is the radius of the planet.  $L = r/R$  is the normalized radial position.  $H$  is the scale height of an equatorially confined plasma sheet.  $m_i$  is the average mass of ions to be transported out.  $n$  is the volume ion number density.  $V_r$  is the radial outflow velocity.  $D_{LL}$  is the diffusion coefficient of the flux tube content of ions. Similarly, the transport equations for heat is of the form

$$q = \frac{3}{2LR} n^{5/3} V_r \frac{d}{dL} (pn^{-5/3}) - \frac{3}{2HR^2L^3} \frac{d}{dL} \left[ \frac{D_{LL}}{L^2} \frac{d}{dL} (nHk_BTL^5) \right], \quad (2)$$

where  $k_B$  is the Boltzmann constant,  $T$  is the ion temperature,  $p = nk_B T$  is the ion pressure,  $q$  is the heating rate density, assumed to be due to the dissipation of MHD turbulence in this paper. On the right hand sides of Eqs. (1) and (2), the first term is due to advection and the second term is due to diffusion. The previous turbulent heating models by Saur (2004) and Ng et al. (2018) can be recovered by keeping only the diffusion terms or the advection terms respectively.

While the scale height  $H$  as a function of  $L$  can be expressed as an empirical formula fitted to observations (Bagenal & Delamere, 2011; Bagenal et al., 2016; Thomsen et al., 2010; Wilson et al., 2017), for simplicity we can approximate it as either a constant such as  $H = 2R$  used by Ng et al. (2018), or a linear function such as  $H = \theta LR$ , with the constant  $\theta = 0.27$ , used by Neupane et al. (2021). We will adopt the latter form in this paper for uniformity, although it is straightforward to derive alternate equations based on other models for the scale height. The ion density is also assumed to have a power law profile of  $n = n_0 L^{-\beta}$ . Following Saur (2004), we will also assume the diffusion coefficient is having a form of power law dependency  $D_{LL} = D_0 L^b$  such that the radial outflow velocity can be solved from Eq. (1) as

$$V_r = \left[ \frac{\dot{M}}{2\pi R m_i} - (\beta - 4) D_0 n_0 \theta L^{b-\beta+1} \right] \frac{1}{\theta R n L^2}. \quad (3)$$

For a diffusion only model without radial outflow, we then have  $b = \beta - 1$  and

$$D_0 = \frac{\dot{M}}{2\pi R m_i (\beta - 4) n_0 \theta}. \quad (4)$$

Note that  $b = \beta$  instead in Saur (2004), which is simply due to assuming a constant  $H$ , rather than the linear form used in this derivation. If  $b = \beta - 1$  is a constant and with Eq. (4),  $V_r$  would be identically zero for all  $L$ , which is in contradiction with the

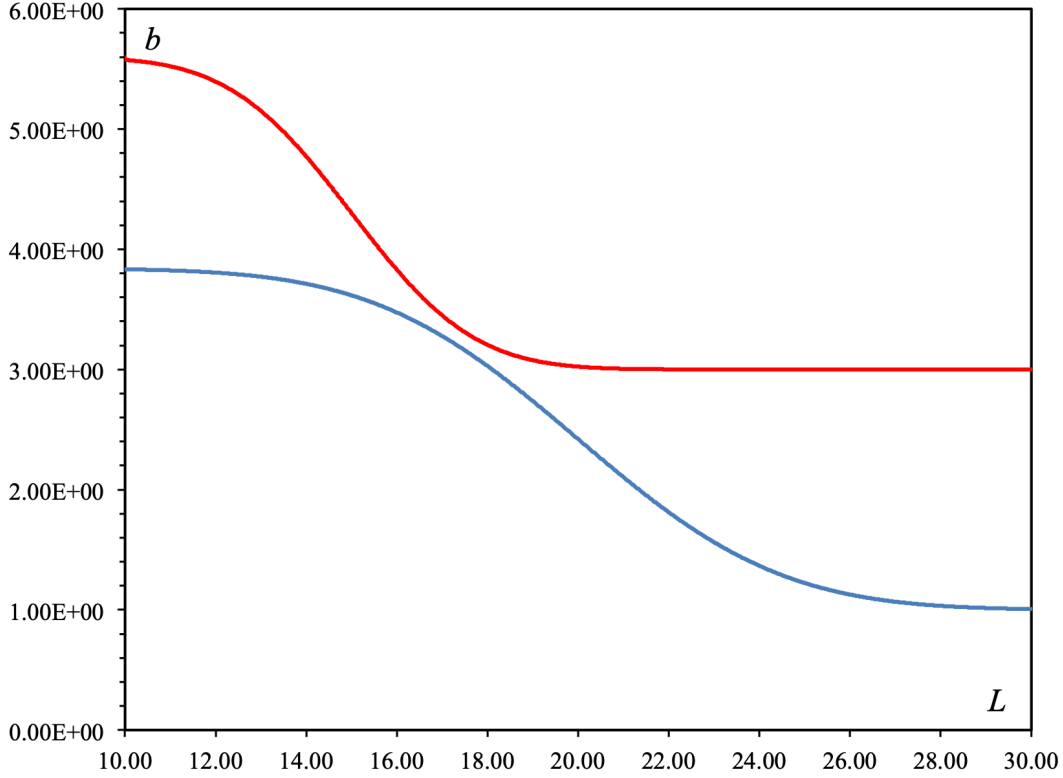


**Figure 1.** The profile of the power law index  $b$  as a function of  $L$  for the Jupiter case (red curve), and the Saturn case (blue curve).

observed growth along  $L$  (e.g., Bagenal & Delamere, 2011). While such a growth in  $V_r$  must be due to a dynamical mechanism, here we will simply model the growth by assuming  $b$  starts decreasing with  $L$  from  $\beta - 1$  (after a certain initial position  $L = L_0$ ) and compare with observations.

Substituting Eq. (3) into Eq. (2), a second order ordinary differential equation for  $T$  can be obtained as

$$\frac{d^2T}{dL^2} - \frac{\eta L^{\beta_1} + \beta_1 - 5}{L} \frac{dT}{dL} - \left[ \frac{2\beta}{3} (\eta L^{\beta_1} - \beta + 4) + (6 - \beta)(\beta_1 - 2) \right] \frac{T}{L^2} = -\xi, \quad (5)$$

where  $\beta_1 = \beta - b - 1$ ,

$$\eta = \frac{\dot{M}}{2\pi R m_i n_0 D_0 \theta} = \beta - 4, \quad (6)$$

and

$$\xi = \frac{2R^2 q L^{\beta-b}}{3k_B n_0 D_0}. \quad (7)$$

Since  $b$  will be chosen to be less than  $\beta - 1$  for larger  $L$ ,  $\beta_1$  is positive when  $V_r$  becomes larger. In this case, terms proportional to  $L^{\beta_1}$  dominate the left hand side of Eq. (5) such that the advection only model by Ng et al. (2018) is recovered when  $L$  is larger. Eq. (5) can be solved as a two-point boundary value problem with  $T(L_0) = T_0$  set for the small  $L$  side. The boundary condition for the large  $L$  side is set by requiring that advection terms are larger than diffusion terms on the left hand side of Eq. (5). Numerically this is imposed by choosing  $T$  on the large  $L$  boundary such that there is no artificial oscillations in  $L$  to make the  $d^2T/dL^2$  term large. From the experience in actually solving

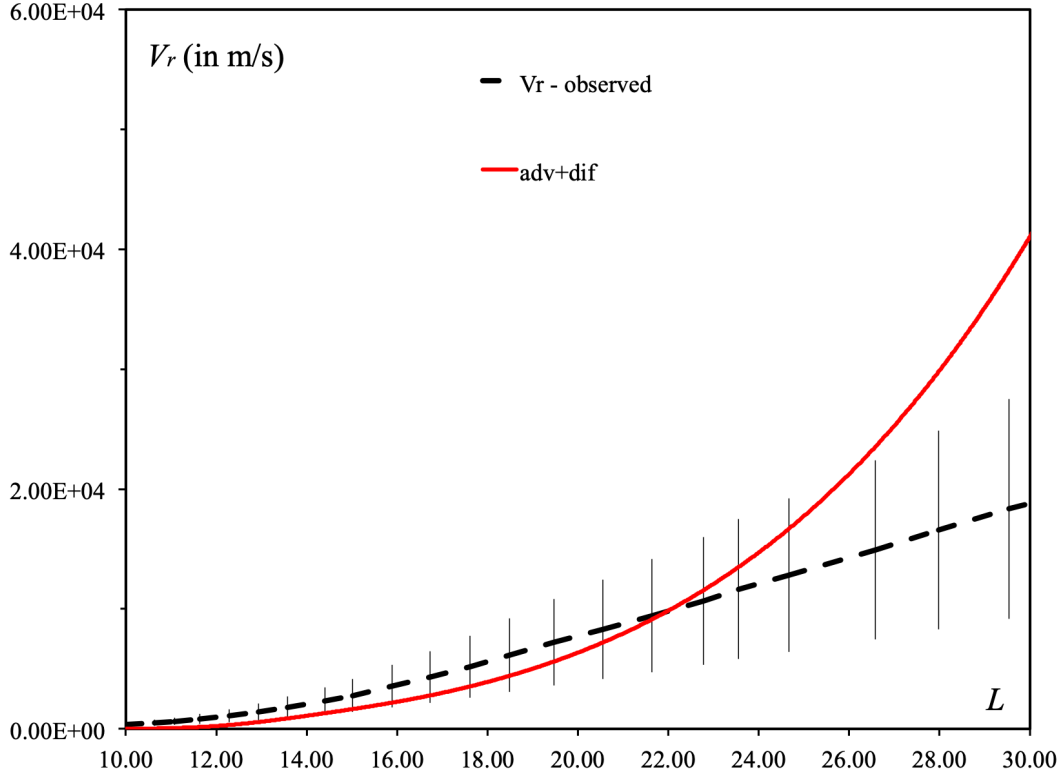


**Figure 2.** Red curve: model output of the radial outflow velocity  $V_r$  as a function of  $L$  for the Jupiter case. Black dashed curve: observed  $V_r$  from Bagenal and Delamere (2011) with  $\pm 50\%$  vertical error bars.

this equation numerically, this can be easily achieved. Much effort has been spent by Kaminker et al. (2017), Ng et al. (2018) and Neupane et al. (2021) to determine the heating rate density  $q$  by analyzing MHD turbulence spectra from magnetometer data for both Saturn and Jupiter. Please refer to these papers for the data analysis methods, as well as various plots showing the distributions of  $q$  as functions of positions. While the resulting  $q$  values scatter over some ranges for different  $L$ , for the purpose of entering  $q$  into the model calculations, it can be approximated by a fitting function of the form  $q = q_0 L^s$ , as obtained by Ng et al. (2018) and Neupane et al. (2021).

### 3 Comparing Model Predictions with Observations

We now apply the new turbulent heating model with both advection and diffusion physics to the Jupiter case using data and parameters used by Ng et al. (2018). Let us first list the values of parameters we use:  $n_0 = 1.9 \times 10^{14} \text{m}^{-3}$ ,  $\beta = 6.6$ ,  $R = R_J = 7 \times 10^7 \text{m}$ ,  $L_0 = 10$ ,  $\dot{M} = 330 \text{kg/s}$ ,  $m_i = 3.2 \times 10^{-26} \text{kg}$ ,  $\theta = 0.27$ ,  $q_0 = 1.2 \times 10^{-14} \text{W/m}^3$ ,  $s = -0.57$ , and  $T_0 = 1.7 \times 10^6 \text{K}$ .

The values of  $L_0$  and  $T_0$  are chosen here to be consistent with our published work. In principle, those values should be determined by physical chemistry models for the inner magnetospheres (Delamere et al., 2005; Fleshman et al., 2013). By such considerations, as well as observations, (e.g., Sittler et al., 2008),  $L_0$  could be chosen slightly inwards to about 8 for Jupiter, and about 7 for Saturn. Such small adjustments should not affect the conclusion of this paper, but might be needed for future investigations.

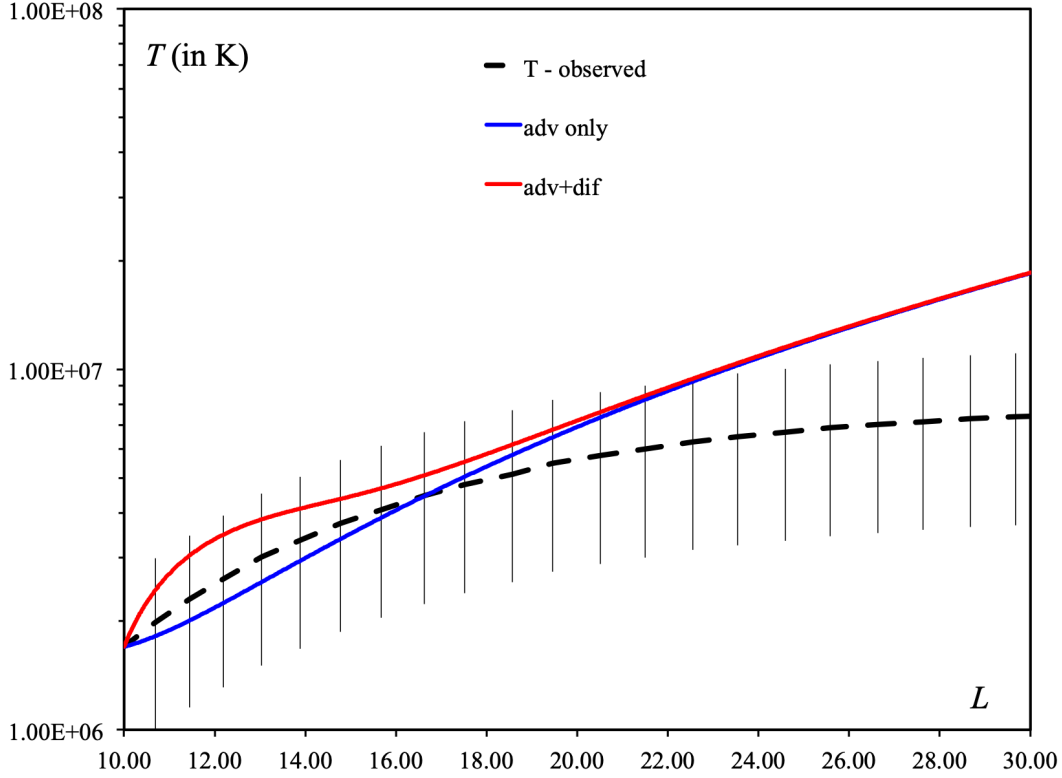


**Figure 3.** Red curve: model output of the ion temperature  $T$  as a function of  $L$  for the Jupiter case. Blue curve: output of  $T$  using the advection only model. Black dashed curve: observed  $T$  from Bagenal and Delamere (2011) with  $\pm 50\%$  vertical error bars.

While there is a considerable amount of freedom to choose the profile of  $b$  as a function of  $L$ , many small adjustments simply produce qualitatively similar results. Therefore we only try a few different profiles and report here just one reasonable case with  $b(L)$  shown as the red curve in Fig. 1. With this choice of  $b$ , the radial outflow velocity can then be calculated using Eqs. (3) and (4), shown as the red curve in Fig. 2. We see that for this profile of  $b$ ,  $V_r$  is mostly within  $\pm 50\%$  of the observed values from Bagenal and Delamere (2011), shown as the black dashed curve, which are derived from Galileo data, interpolated for the specific  $\dot{M}$  value used in this calculation. The model  $V_r$  does get higher than the observed values as  $L$  getting near 30 when the heating model is expected to start failing.

The corresponding ion temperature  $T$  can then be calculated using Eq. (5), shown as the red curve in Fig. 3. The blue curve in Fig. 3 shows  $T$  calculated using the advection only model, i.e., keeping only terms proportional to  $L^{\beta_1}$  on the left hand side of Eq. (5). We see that the output from the combined model shows a much faster increase from  $T_0$  than the advection only model. Then the two models actually give virtually the same  $T$  after  $L \sim 20$ . Overall, the output from the advection only model is well within a factor of two of the output from the combined model. This provides a justification that the advection only model used by Ng et al. (2018) is valid, as long as the radial outflow velocity begins to grow larger. Also shown as the black dashed curve in Fig. 3 is the observed  $T$ , again from Bagenal and Delamere (2011). We see that the predicted  $T$  from both models actually fall within  $\pm 50\%$  of the observed values for over half of the range shown. The predicted  $T$  becomes consistently larger than the observations further in the  $L$  range but is still within a factor of three.

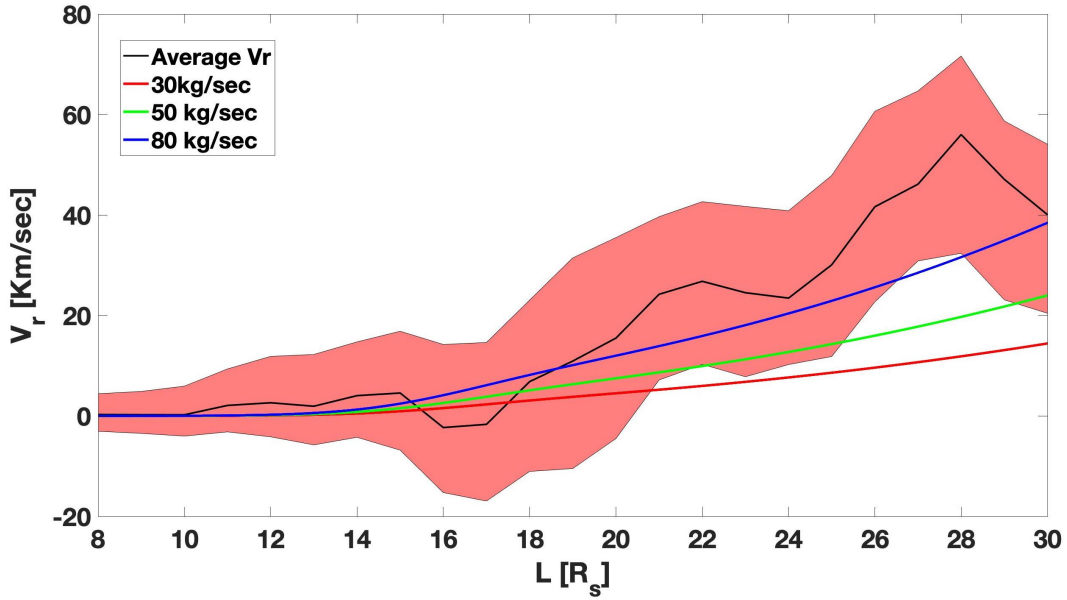


**Figure 4.** Red, green, and blue curves: model outputs of the radial outflow velocity  $V_r$  as a function of  $L$  for the Saturn case using  $\dot{M} = 30, 50,$  and  $80$  kg/s. Black curve: observed  $V_r$  from Wilson et al. (2017) with the shaded area indicating values between 25th and 75th percentile.

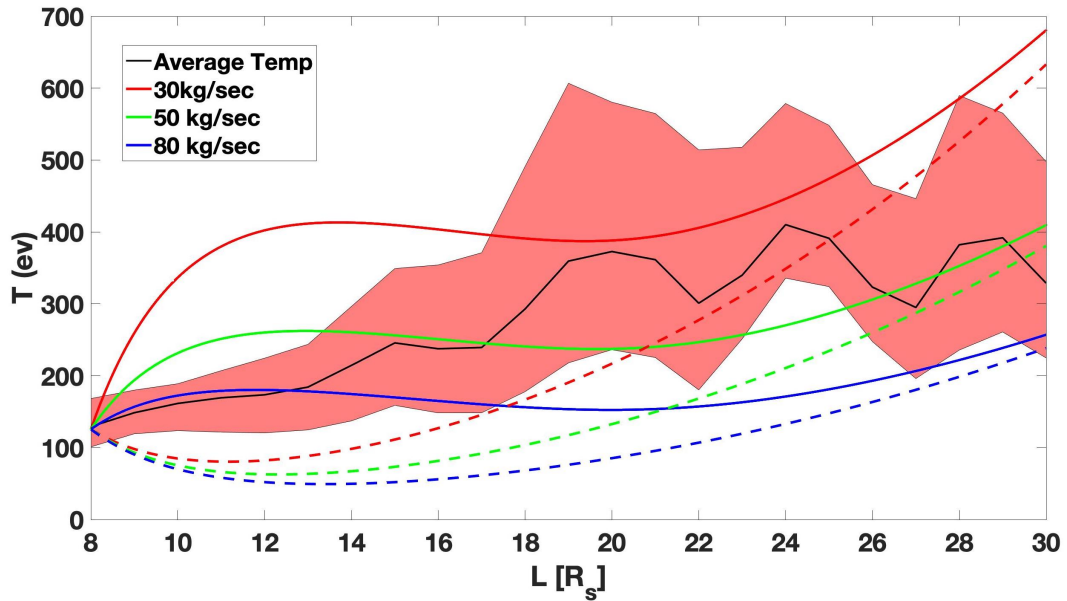


**Figure 5.** Red, green, and blue curves: model outputs of the ion temperature  $T$  as a function of  $L$  for the Saturn case using  $\dot{M} = 30, 50,$  and  $80$  kg/s, with solid curves from the combined model, and dashed curves from the advection only model. Black curve: observed  $T$  from Wilson et al. (2017) with the shaded area indicating values between 25th and 75th percentile.

Let us now apply the same model to the Saturn case using data and parameters used by Neupane et al. (2021). Let us first list the values of parameters we use:  $n_0 = 1.79 \times 10^{11} \text{m}^{-3}$ ,  $\beta = 4.84$ ,  $R = R_S = 6 \times 10^7 \text{m}$ ,  $L_0 = 8$ ,  $m_i = 3 \times 10^{-26} \text{kg}$ ,  $\theta = 0.27$ ,  $q_0 = 2.51 \times 10^{-16} \text{m}^3/\text{W}$ ,  $s = -0.3$ , and  $T_0 = 125.6 \text{eV}$ . As in the Jupiter case, a  $b$  profile is chosen after a few trials to give reasonable  $V_r$  profiles, shown as the blue curve in Fig. 1. It has values quite different from the Jupiter case since the  $\beta$  values are different. Due to some uncertainty in the value of  $\dot{M}$  (Delamere & Bagenal, 2013; Fleshman et al., 2013), three values, 30, 50, and 80 kg/s, are used, as in Neupane et al. (2021). The  $V_r$  profiles for these three cases calculated from Eqs. (3) and (4) are shown in Fig. 4 as the red, green, and blue curves respectively. We see that while the blue curve seems to be closest to the observed values (black curve) from Wilson et al. (2017), the green curve is still mainly within the uncertainty region (the shaded area indicating values between 25th and 75th percentile). Only the red curve is significantly below observations.

The corresponding ion temperature  $T$  calculated from Eq. (5) are shown in Fig. 5 for the same three  $\dot{M}$  cases as the red, green, and blue curves. The observed temperature shown as the black curve is again from Wilson et al. (2017). We see that the green solid curve fits the observations the best, while the red solid curve is significantly higher, and the blue solid curve is significantly lower. Combining both the  $V_r$  and  $T$  comparisons, the case for the green curves, or  $\dot{M} = 50 \text{kg/s}$ , seems to give an overall satisfactory predictions. In Fig. 5 we have also plotted predictions using the advection only model as dashed curves, with the same color for each  $\dot{M}$  case. Comparing with those curves, the combined model again gives a much faster increase of  $T$  starting from  $L_0$ , instead of having initial decreases, which now fits much better with observations, while the predictions at larger  $L$  are essentially at the same levels. Therefore the Saturn case again shows that the combined model indeed provides better agreement, and also recovers the advection only model for larger  $L$ .

## 4 Conclusion

In this paper, we have developed the formulation for a one-dimensional steady-state turbulent heating model for the inner magnetospheres of giant planets, by combining both the diffusion and advection effects. Combining these effects into a single model provides a better theoretical foundation than either the diffusion only or advection only approaches of Saur (2004), and Ng et al. (2018) respectively. This is because the new model will consistently have the diffusion effects being dominant when the radial outflow speed  $V_r$  is small, but will change to advection effects being dominant when  $V_r$  is larger. In practice, we also show that the combined model does give better comparisons with observations of both  $V_r$ , and the ion temperature  $T$ , by repeating the studies done previously for Jupiter by Ng et al. (2018), and for Saturn by Neupane et al. (2021). The new calculations from the combined model also provide a justification for the advection only model for the use in larger radial positions  $L$  when  $V_r$  has increased substantially, since the two models give almost the same outputs for larger  $L$ . With this new model and the comparisons with observations, there is more confidence that MHD turbulence can indeed provide enough heating to explain the increase with ion temperature in the inner magnetospheres of the giant planets.

While this turbulent heating model is now on firmer ground, it is still far from being a dynamical model, since we have not included an equation of motion that can provide a mechanism for the increase of  $V_r$ . Rather, we have simply tuned the model to better compare with observed profiles of  $V_r$  and  $T$ . Such a study is obviously a worthwhile future research direction, but is outside the scope of this paper. We additionally neglect other effects which contribute to the beginning of the break down of the model after about  $L = 30$  such as the beginning of the breakdown of corotation, and the return of flux tubes, as well as other possible heat loss mechanisms. Therefore, there are several potential directions that can be taken to facilitate further improvement of the model.

## Acknowledgments

This work is supported by NASA grant 80NSSC20K1279.

## Data Availability Statement

The new model outputs in this paper is based on parameters from previous data analysis in the papers by Ng et al. (2018) and Neupane et al. (2021). Please refer to these two papers for the availability of data used in those studies.

## References

- Bagenal, F., & Delamere, P. A. (2011, May). Flow of mass and energy in the magnetospheres of Jupiter and Saturn. *Journal of Geophysical Research (Space Physics)*, *116*(A15), 5209. doi: 10.1029/2010JA016294
- Bagenal, F., Wilson, R. J., Siler, S., Paterson, W. R., & Kurth, W. S. (2016). Survey of galileo plasma observations in jupiter's plasma sheet. *Journal of Geophysical Research: Planets*, n/a–n/a. Retrieved from <http://dx.doi.org/10.1002/2016JE005009> (2016JE005009) doi: 10.1002/2016JE005009
- Delamere, P. A., & Bagenal, F. (2010, October). Solar wind interaction with Jupiter's magnetosphere. *Journal of Geophysical Research (Space Physics)*, *115*(A14), 10201+. doi: 10.1029/2010JA015347
- Delamere, P. A., & Bagenal, F. (2013, November). Magnetotail structure of the giant magnetospheres: Implications of the viscous interaction with the solar wind. *Journal of Geophysical Research (Space Physics)*, *118*, 7045-7053. doi: 10.1002/2013JA019179
- Delamere, P. A., Bagenal, F., & Steffl, A. (2005, December). Radial variations in the Io plasma torus during the Cassini era. *Journal of Geophysical Research (Space Physics)*, *110*, 12223+. doi: 10.1029/2005JA011251
- Fleshman, B. L., Delamere, P. A., Bagenal, F., & Cassidy, T. (2013, August). A 1-D model of physical chemistry in Saturn's inner magnetosphere. *Journal of Geophysical Research (Planets)*, *118*, 1567-1581. doi: 10.1002/jgre.20106
- Hill, T. W., Dessler, A. J., & Goertz, C. K. (1983). Magnetospheric Models. In A. J. Dessler (Ed.), *Physics of the jovian magnetosphere* (p. 353-394).
- Kaminker, V., Delamere, P. A., Ng, C. S., Dennis, T., Otto, A., & Ma, X. (2017, April). Local time dependence of turbulent magnetic fields in Saturn's magnetodisc. *Journal of Geophysical Research (Space Physics)*, *122*, 3972-3984. doi: 10.1002/2016JA023834
- Neupane, B. R., Delamere, P. A., Ma, X., Ng, C.-S., Burkholder, B., & Damiano, P. (2021). On the nature of turbulent heating and radial transport in saturn's magnetosphere. *Journal of Geophysical Research: Space Physics*, *126*(1), e2020JA027986. Retrieved from <https://agupubs.onlinelibrary.wiley.com/doi/abs/10.1029/2020JA027986> (e2020JA027986 2020JA027986) doi: <https://doi.org/10.1029/2020JA027986>
- Ng, C. S., Bhattacharjee, A., Munsu, D., Isenberg, P. A., & Smith, C. W. (2010, February). Kolmogorov versus Iroshnikov-Kraichnan spectra: Consequences for ion heating in the solar wind. *J. Geophys. Res.*, *115*, 2101. doi: 10.1029/2009JA014377
- Ng, C. S., Delamere, P. A., Kaminker, V., & Damiano, P. A. (2018). Radial transport and plasma heating in jupiter's magnetodisc. *Journal of Geophysical Research: Space Physics*, *123*(8), 6611-6620. Retrieved from <https://agupubs.onlinelibrary.wiley.com/doi/abs/10.1029/2018JA025345> doi: 10.1029/2018JA025345
- Saur, J. (2004, February). Turbulent Heating of Jupiter's Middle Magnetosphere. *Astrophys. J. Lett.*, *602*, L137-L140. doi: 10.1086/382588
- Sittler, E., Andre, N., Blanc, M., Burger, M., Johnson, R., Coates, A., . . . Young, D. (2008). Ion and neutral sources and sinks within saturn's inner magne-

- tosphere: Cassini results. *Planetary and Space Science*, 56(1), 3-18. Retrieved from <https://www.sciencedirect.com/science/article/pii/S0032063307002309> (Surfaces and Atmospheres of the Outer Planets, their Satellites and Ring Systems: Part III) doi: <https://doi.org/10.1016/j.pss.2007.06.006>
- Thomsen, M. F., Reisenfeld, D. B., Delapp, D. M., Tokar, R. L., Young, D. T., Crary, F. J., . . . Williams, J. D. (2010, October). Survey of ion plasma parameters in Saturn's magnetosphere. *Journal of Geophysical Research (Space Physics)*, 115, 10220-+. doi: 10.1029/2010JA015267
- Wilson, R. J., Bagenal, F., & Persoon, A. M. (2017). Survey of thermal plasma ions in saturn's magnetosphere utilizing a forward model. *Journal of Geophysical Research: Space Physics*, 122(7), 7256-7278. Retrieved from <https://agupubs.onlinelibrary.wiley.com/doi/abs/10.1002/2017JA024117> doi: 10.1002/2017JA024117